

Supporting Information

Effects of single α -to- β residue replacements on recognition of an extended segment in a viral fusion protein

Victor K. Outlaw¹, Dale F. Kreidler¹, Debora Stelitano^{2,3,4}, Matteo Porotto^{2,3,4*}, Anne Moscona^{2,3,5,6*}, Samuel H. Gellman^{1*}

¹Department of Chemistry, University of Wisconsin, Madison, Wisconsin, 53706, United States

²Department of Pediatrics, Columbia University Medical Center, New York, New York, 10032, United States

³Center for Host–Pathogen Interaction, Columbia University Medical Center, New York, New York, 10032, United States

⁴Department of Experimental Medicine, University of Campania ‘Luigi Vanvitelli’, Italy

⁵Department of Microbiology & Immunology, Columbia University Medical Center, New York, New York, 10032, United States

⁶Department of Physiology & Cellular Biophysics, Columbia University Medical Center, New York, New York, 10032, United States

* Corresponding Authors. Address correspondence to: Samuel H. Gellman, gellman@chem.wisc.edu; Anne Moscona, am939@cumc.columbia.edu; Matteo Porotto, mp3509@cumc.columbia.edu

Table of Contents

Peptide Synthesis and Purification	3
Instrumentation	3
General Procedure	3
Assessment of Peptide Efficacy	15
Plasmids, Cells, and Viruses	15
Antiviral Efficacy against Live RSV or HPIV3	15
X-ray Crystallography	16
Crystallization Conditions	16
X-ray Data Collection	16
Data Processing, Structure Solution, and Refinement	17
References	23

Peptide Synthesis and Purification

Instrumentation

Solid-phase peptide synthesis was performed on a CEM MARS microwave reactor using polypropylene syringes fitted with a porous disc (Torviq). Preparative HPLC was performed using a Shimadzu HPLC system (SCL-10VP system controller, LC-6AD pumps, SIL-10ADVP autosampler, SPD-10VP UV-vis detector, FRC-10A fraction collector) equipped with a Waters XSelect CSH Prep C18 column (5 μm particle size, 19 mm \times 250 mm). Peptide purity measurements were performed on a Waters Acquity H-Class UPLC equipped with an Acquity UPLC BEH C18 column (130 \AA pore size, 1.7 μm particle size, 2.1 mm \times 50 mm). Mass spectra were obtained on a Bruker microflex LRF MALDI-TOF-MS. Circular dichroism experiments were performed on an Aviv Biomedical model 420 CD spectrometer.

Table S1 Instrumentation used for peptide characterization

Instrument Name	Instrument Type	Grant
Waters Acquity H-Class	UPLC	DARPA N66001-15-2-4023
Bruker microflex LRF	MALDI-TOF-MS	Generous gift from the Bender Fund
Aviv Biomedical model 420	CD spectrometer	NIH R01GM061238

General Procedure

Peptides were prepared on Rink amide resin using microwave-assisted solid-phase peptide synthesis (MA-SPPS). Resin was purchased from Millipore–Sigma. Fmoc- α -amino acids, Fmoc- β -amino acids, Fmoc-N-methyl-serine, and coupling reagents were purchased from Chem-Impex International. Protected Fmoc- α -amino acids included: Asp(*t*-Bu ester), Glu(*t*-Bu ester), His(trityl), Lys(Boc), Asn(trityl), Gln(trityl), Arg(Pbf), Ser(*t*-Bu ether), Thr(*t*-Bu ether), Trp(Boc), and Tyr(*t*-Bu ether). Protected Fmoc- β^3 -amino acids included: β^3 -homoaspartic acid (*t*-Bu ester).

Rink amide resin was pre-swelled with DMF in a polypropylene fritted syringe, then drained and washed with DMF. Coupling reactions were performed using solutions comprised of 4 equivalents Fmoc-amino acid, 4 equivalents of 1-[bis(dimethylamino)methylene]-1H-1,2,3-triazolo[4,5-b]pyridinium 3-oxide hexafluorophosphate (HATU), and 8 equivalents of diisopropylethylamine (DIEA) in biotechnology-grade dimethylformamide (DMF) at a final concentration of 100 mM Fmoc-amino acid. Coupling reactions were carried out by microwave-assisted synthesis using a 2 min ramp to

70 °C followed by a 4 min hold at 70 °C. Deprotection was effected by addition of 20% (v/v) piperidine in biotechnology-grade DMF. The deprotection reactions were carried out by microwave-assisted synthesis using a 2 min ramp to 80 °C followed by a 2 min hold at 80 °C. The resin was washed with 3–5 resin volumes of biotechnology-grade DMF after each coupling and deprotection reaction.

The synthesis of HPIV3 HRN and RSV HRN was performed as previously described.¹ The use of pseudoproline dipeptides (Millipore-Sigma, underlined in the sequences below) incorporated at strategic positions throughout the sequence was necessary for successful syntheses.

HPIV3 HRN: Ac-QARSDIEKLKEAIRDTNKAVQSVQSSIGNLIVAIKSVQDYVNKEIVPSIAR-NH₂

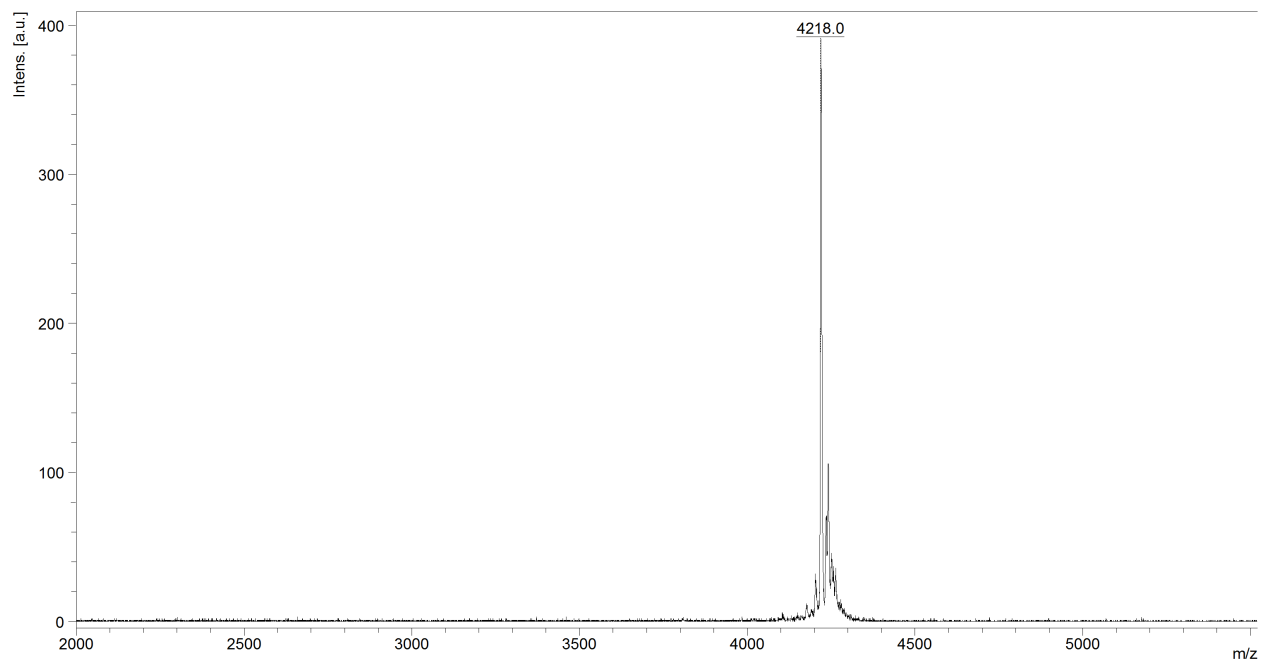
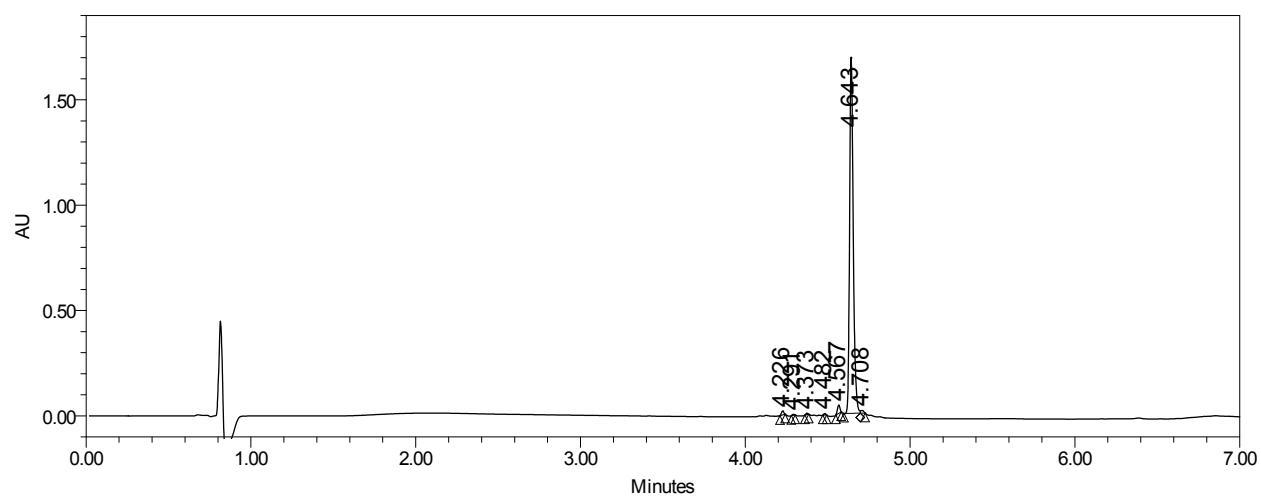
RSV HRN: Ac-HLEGEVNKIKSALLSTNKAVSLSNGSVLTSKVLDLKNYIDKQLLPVVK-NH₂

Following the final deprotection step, the N-terminus of the peptide was capped by stirring the resin in 8:2:1 DMF:DIEA:Ac₂O at 23 °C for 30 minutes. The resin was washed with DMF (3 × 25 mL) and DCM (3 × 25 mL), and peptide cleavage from resin was effected by mixing with a solution of 94% TFA, 2.5% ethanedithiol, 2.5% H₂O, and 1% triisopropylsilane for 3 hours. The resulting solution was filtered through the fritted syringe, the remaining resin was washed with 2–3 column volumes of TFA, and the combined extracts were concentrated under N₂. The peptide was precipitated by addition of cold diethyl ether, pelleted by centrifugation, and dried under N₂ to afford the crude product as a powder. Purification of peptides was achieved by reverse-phase HPLC on a semi-preparative C18 column using a gradient of water (+0.1% TFA) and acetonitrile (+0.1% TFA). The identity of each peptide was confirmed by MALDI-TOF mass spectrometry. Purity was established by peak area integration of reverse phase UPLC chromatograms using a 10–95% H₂O/MeCN (+0.1% TFA) gradient over 6 minutes (Figures S1–S18).

VIQKI V449(β^3 V)Sequence: Ac-(β^3 V)ALDPIDISIVLNKIKSQLEESKEWIRRSNKILDSI-NH₂

Calculated monoisotopic [M+H]: 4218.4

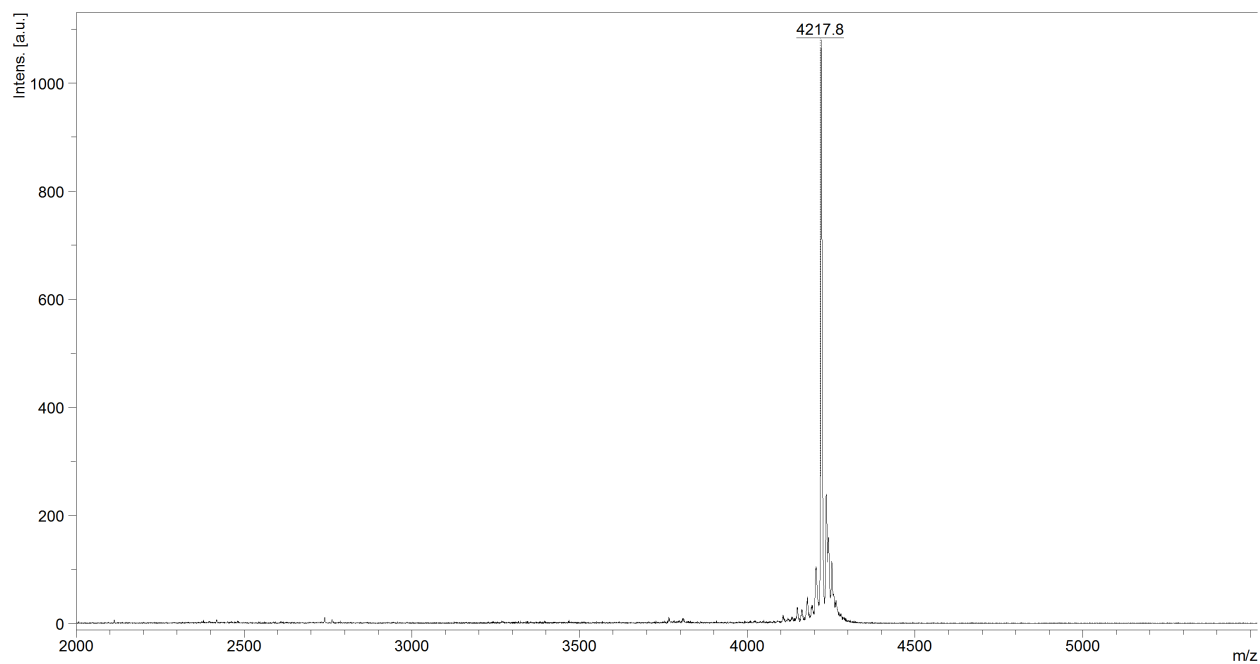
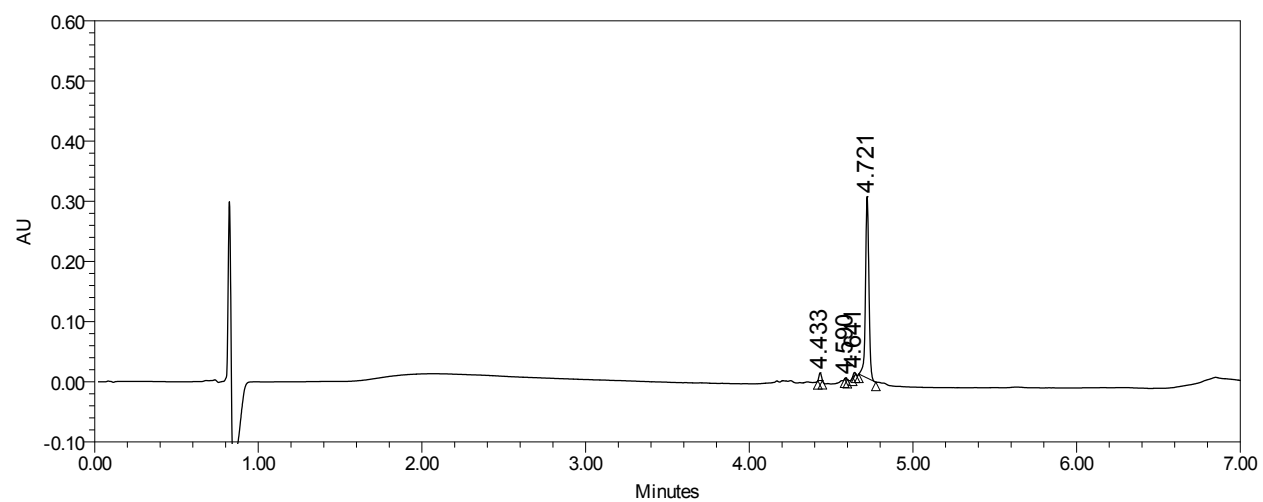
Calculated monoisotopic [M+2H]: 2109.7

Figure S1. VIQKI V449(β^3 V) MALDI-TOF MS analysisFigure S2. VIQKI V449(β^3 V) UPLC purity analysis, UPLC gradient from 10-95% MeCN/H₂O over 6 minutes (0.3 mL/min; column- Waters Acquity BEH C4 1.7 μ m, 2.1 x 100 mm, purity >95%)

VIQKI A450(β^3 A)Sequence: Ac-V(β^3 A)LDPIDISIVLNKIKSQLEESKEWIRRSNKILDSI-NH₂

Calculated monoisotopic [M+H]: 4218.4

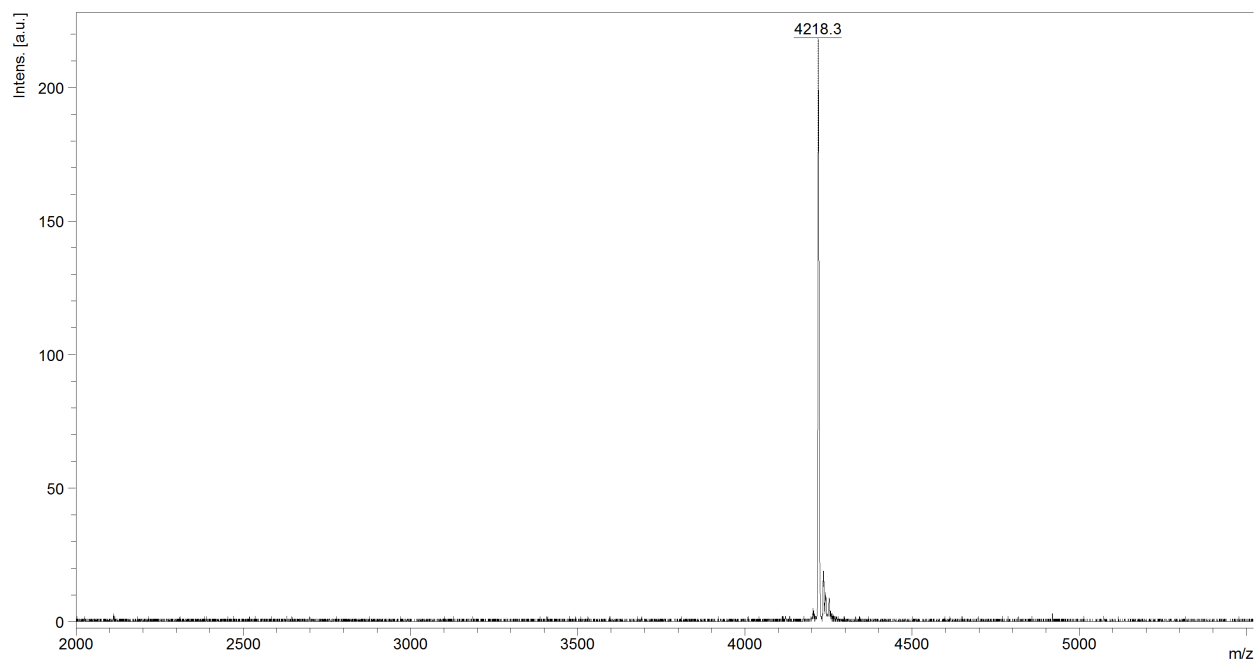
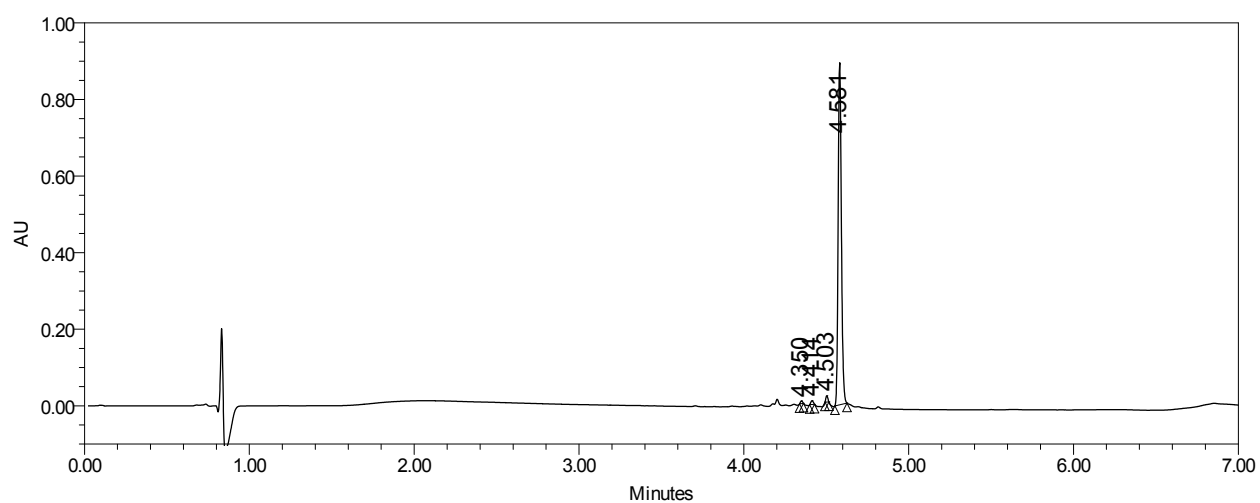
Calculated monoisotopic [M+2H]: 2109.7

Figure S3. VIQKI A450(β^3 A) MALDI-TOF MS analysisFigure S4. VIQKI A450(β^3 A) UPLC purity analysis, UPLC gradient from 10-95% MeCN/H₂O over 6 minutes (0.3 mL/min; column- Waters Acquity BEH C4 1.7 μ m, 2.1 x 100 mm, purity >95%)

VIQKI L451(β^3 L)Sequence: Ac-VA(β^3 L)DPIDISIVLNKIKSQLEESKEWIRRSNKILDSI-NH₂

Calculated monoisotopic [M+H]: 4218.4

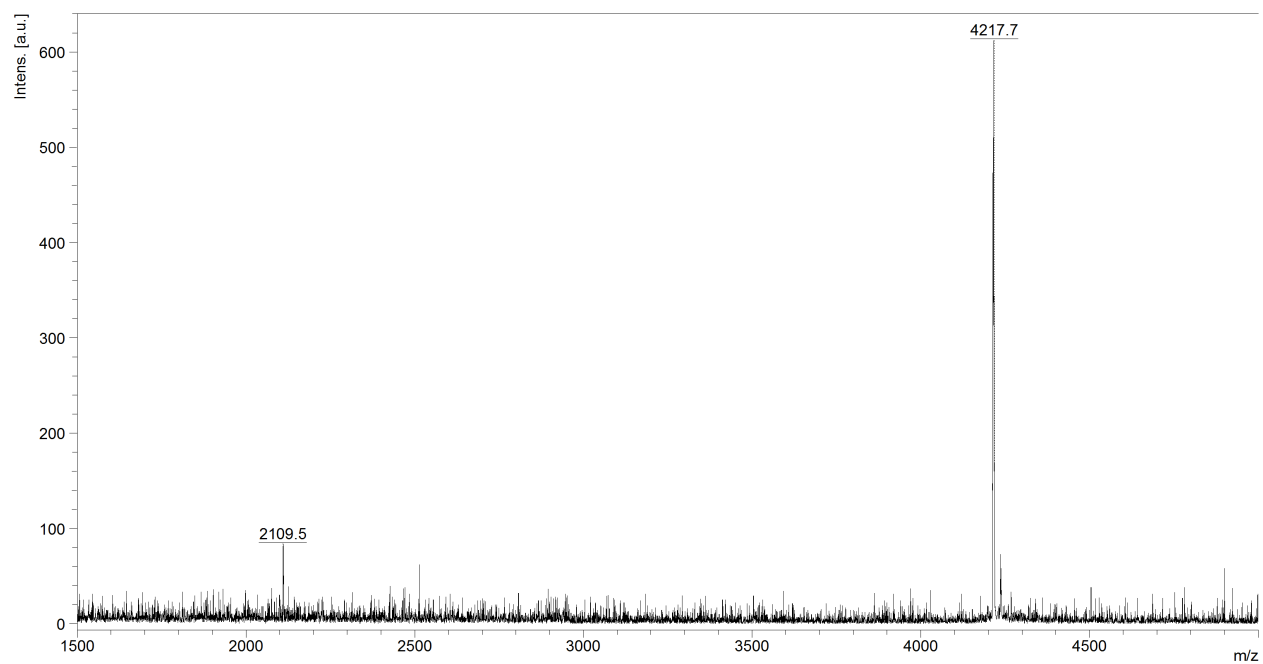
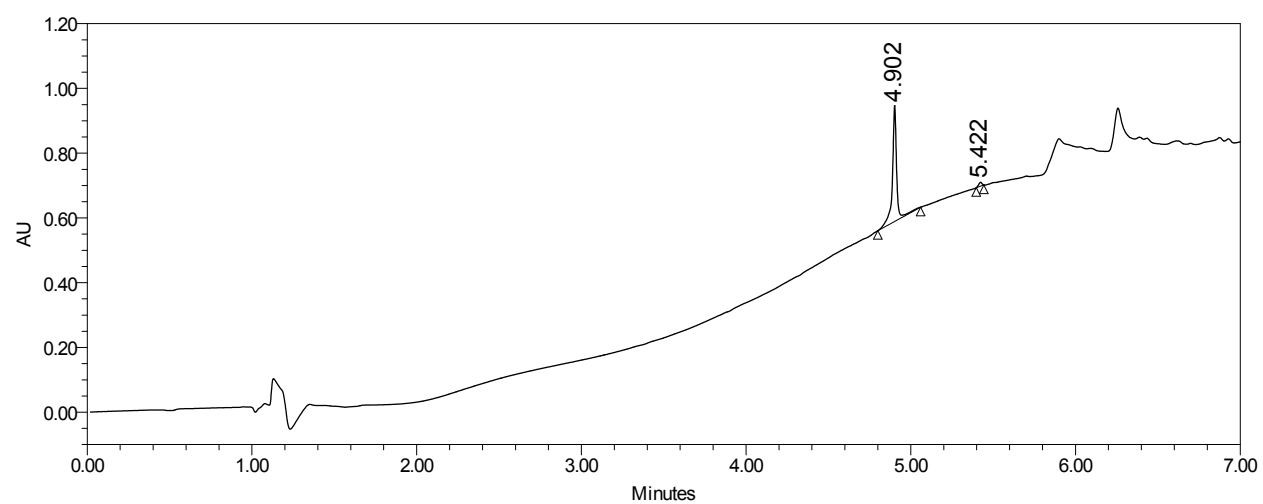
Calculated monoisotopic [M+2H]: 2109.7

Figure S5. VIQKI L451(β^3 L) MALDI-TOF MS analysisFigure S6. VIQKI L451(β^3 L) UPLC purity analysis, UPLC gradient from 10-95% MeCN/H₂O over 6 minutes (0.3 mL/min; column-Waters Acquity BEH C4 1.7 μ m, 2.1 x 100 mm, purity >95%)

VIQKI D452(β^3 D)Sequence: Ac-VAL(β^3 D)PIDISIVLNKIKSQLEESKEWIRRSNKILDSI-NH₂

Calculated monoisotopic [M+H]: 4218.4

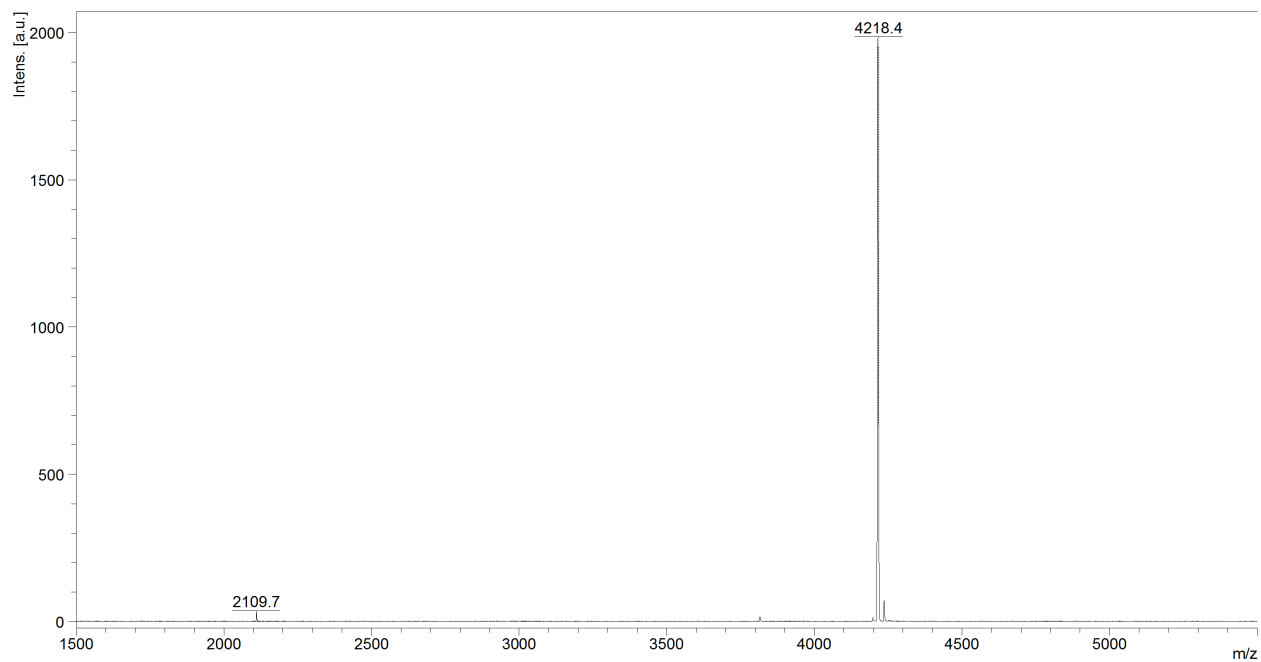
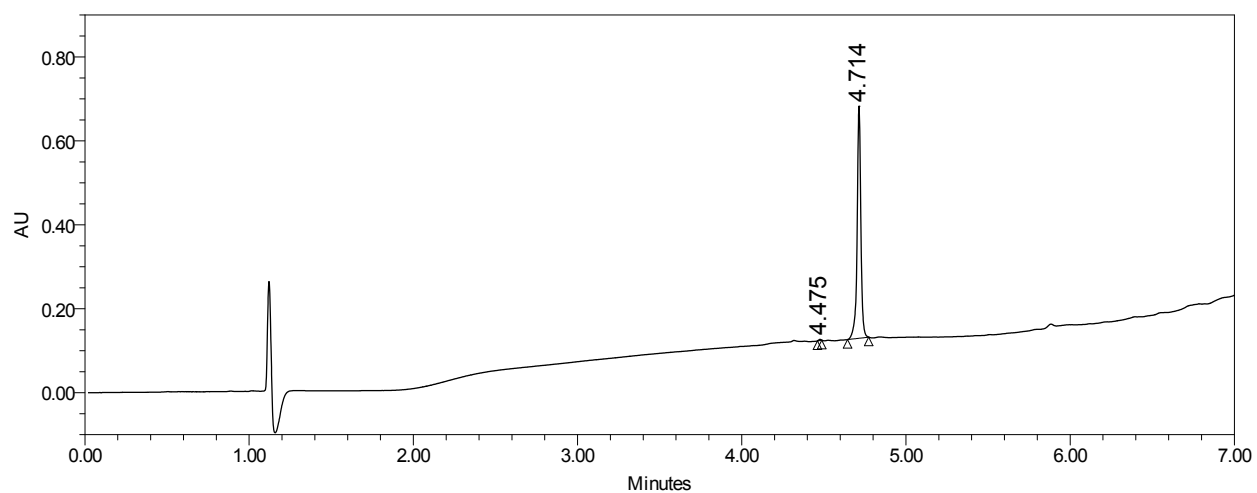
Calculated monoisotopic [M+2H]: 2109.7

Figure S7. VIQKI D452(β^3 D) MALDI-TOF analysisFigure S8. VIQKI D452(β^3 D) UPLC purity analysis, UPLC gradient from 10-95% MeCN/H₂O over 6 minutes (0.3 mL/min; column- Waters Acquity BEH C4 1.7 μ m, 2.1 x 100 mm, purity >95%)

VIQKI P453($\beta^3\text{P}$)Sequence: Ac-VALD($\beta^3\text{P}$)IDISIVLNKIKSQLEESKEWIRRSNKILDSI-NH₂

Calculated monoisotopic [M+H]: 4218.4

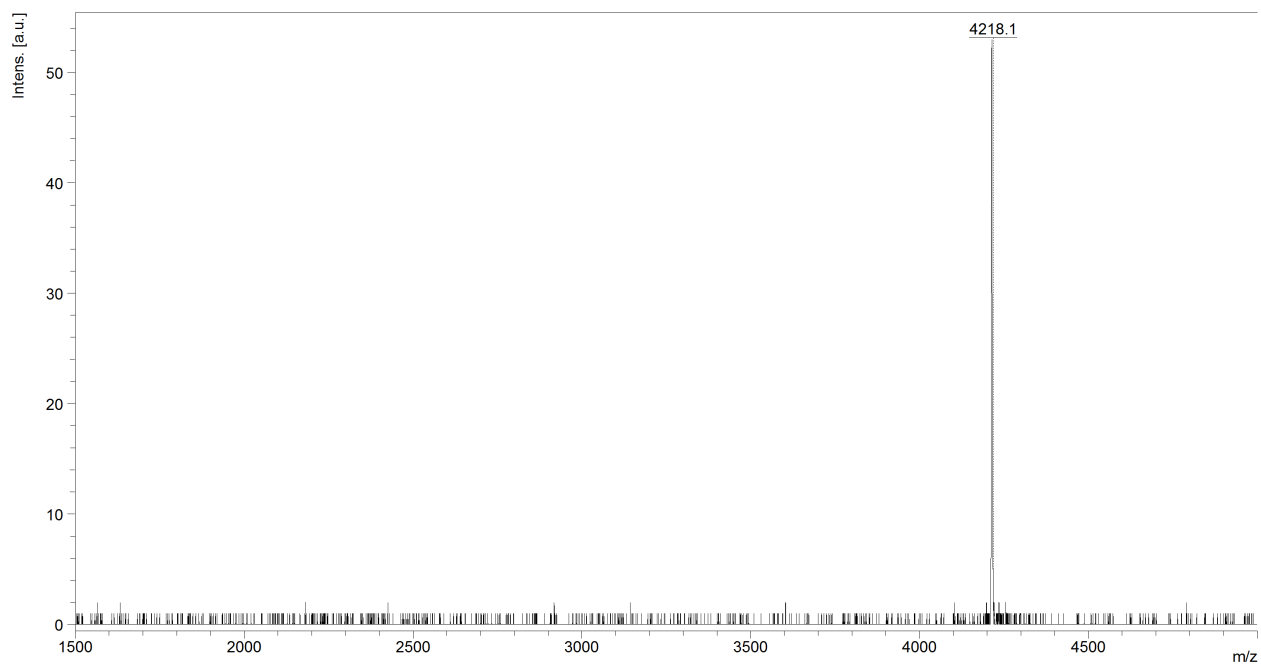
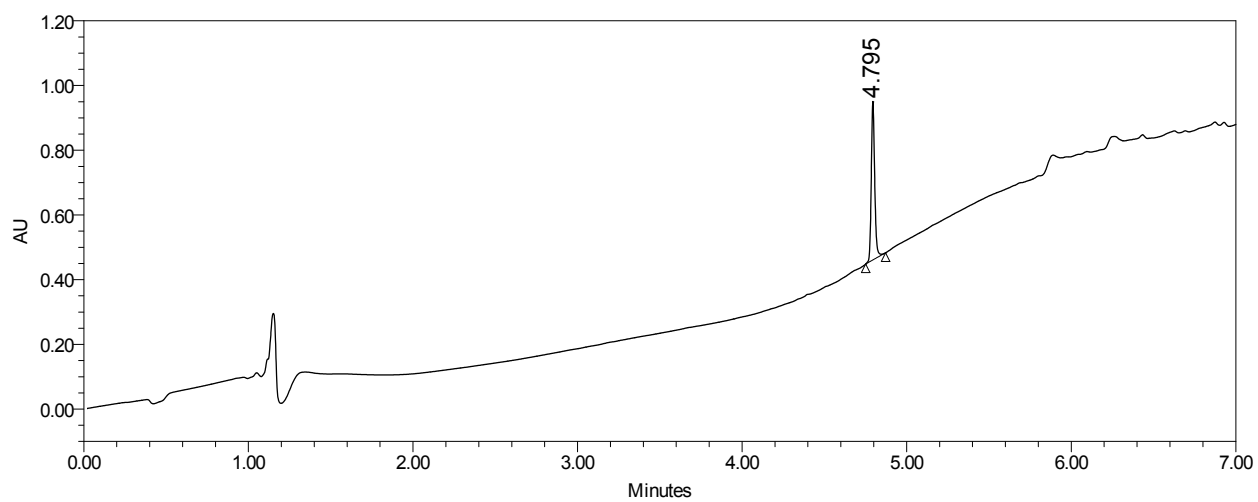
Calculated monoisotopic [M+2H]: 2109.7

Figure S9. VIQKI P453($\beta^3\text{P}$) MALDI-TOF MS analysisFigure S10. VIQKI P453($\beta^3\text{P}$) UPLC purity analysis, UPLC gradient from 10-95% MeCN/H₂O over 6 minutes (0.3 mL/min; column- Waters Acquity BEH C4 1.7 μm , 2.1 x 100 mm, purity >95%)

VIQKI I454(β^3 I)Sequence: Ac-VALDP(β^3 I)DISIVLNKIKSQLEESKEWIRRSNKILDSI-NH₂

Calculated monoisotopic [M+H]: 4218.4

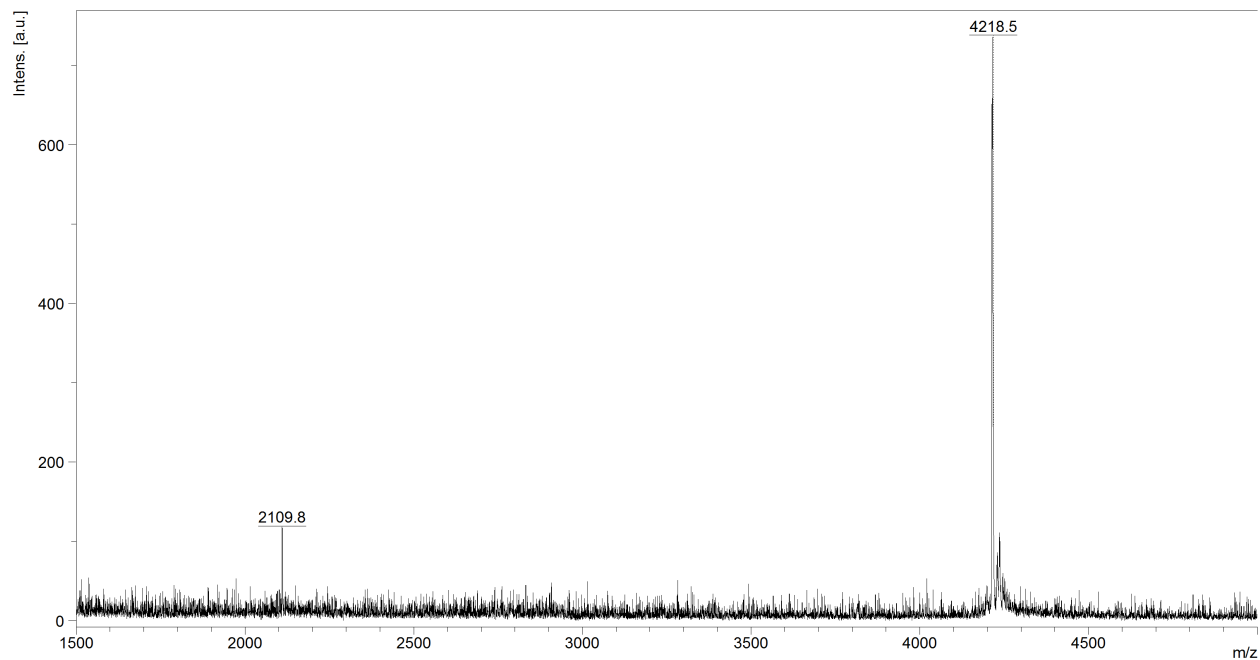
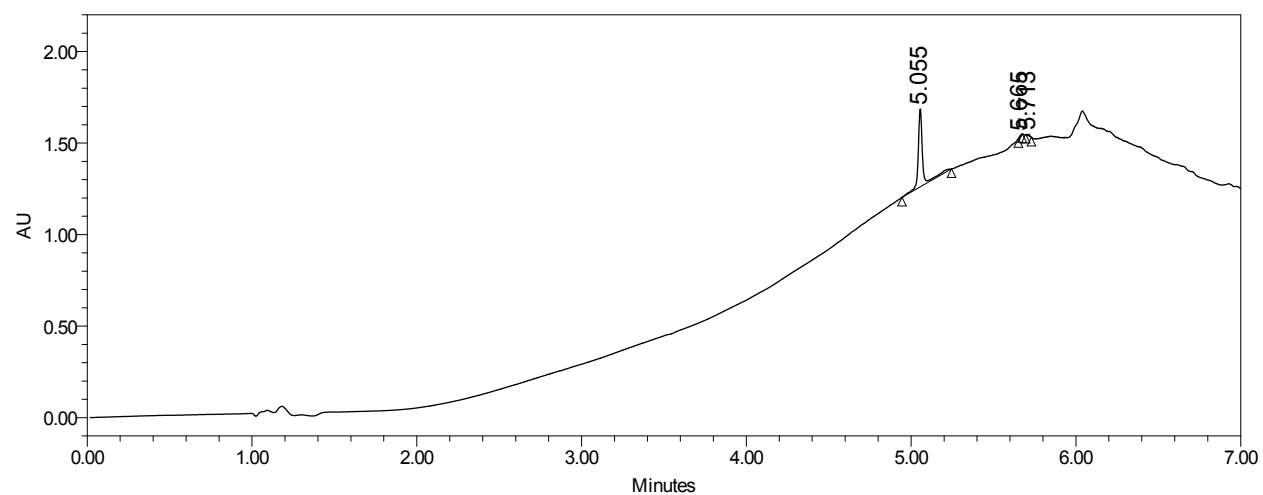
Calculated monoisotopic [M+2H]: 2109.7

Figure S11. VIQKI I454(β^3 I) MALDI-TOF MS analysisFigure S12. VIQKI I454(β^3 I) UPLC purity analysis, UPLC gradient from 10-95% MeCN/H₂O over 6 minutes (0.3 mL/min; column- Waters Acquity BEH C4 1.7 μ m, 2.1 x 100 mm, purity >95%)

VIQKI D455(β^3 D)Sequence: Ac-VALDPI(β^3 D)ISIVLNKIKSQLEESKEWIRRSNKILDSI-NH₂

Calculated monoisotopic [M+H]: 4218.4

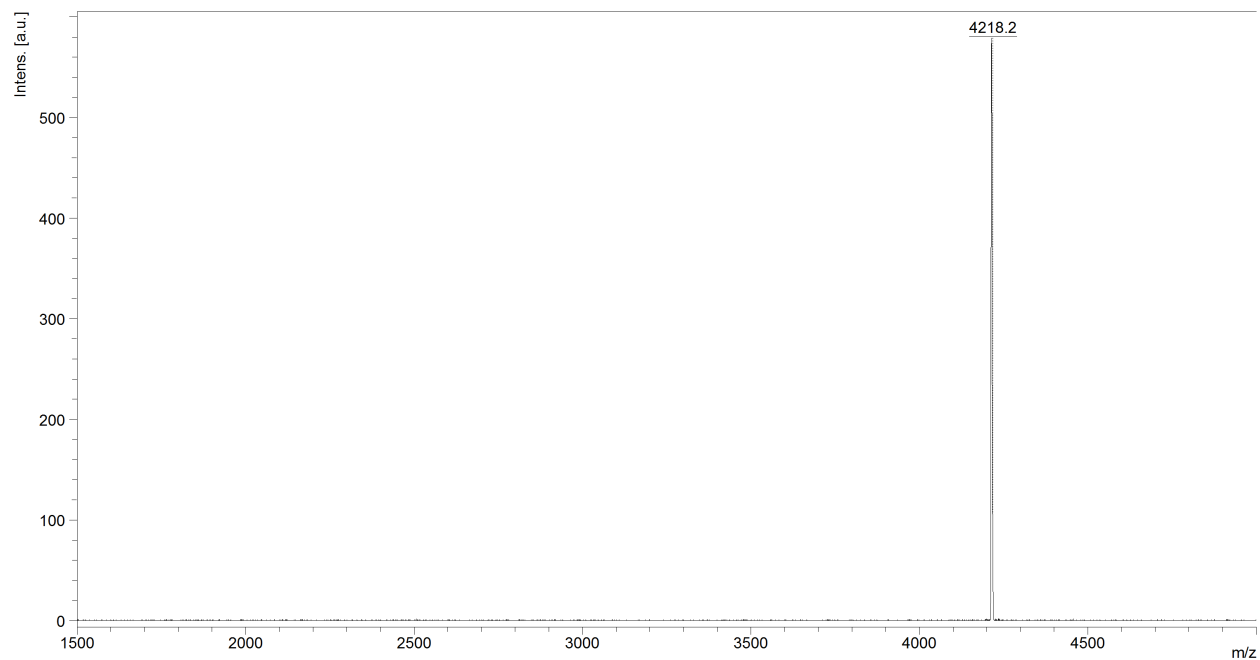
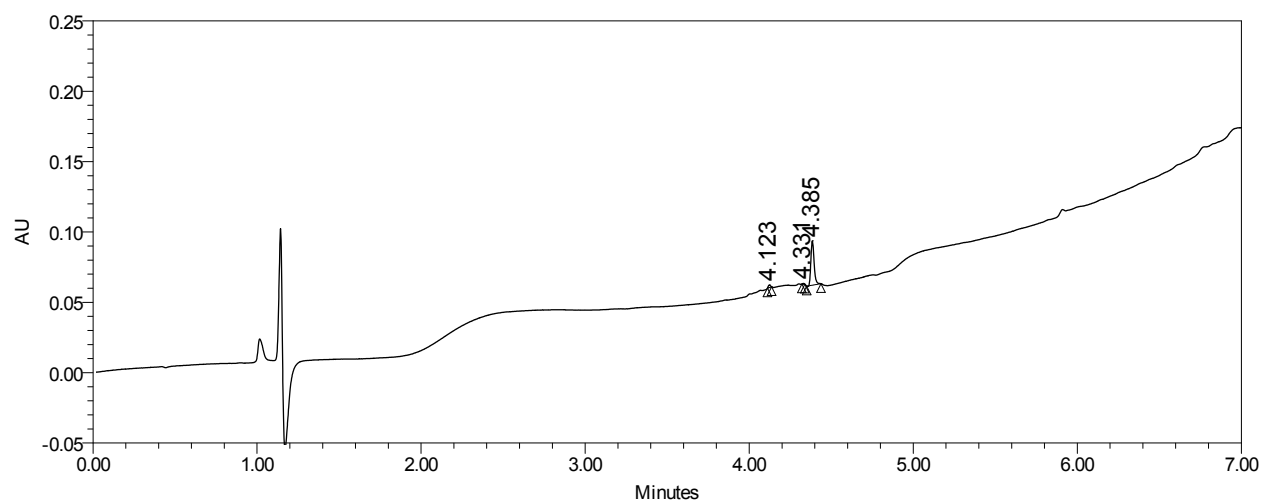
Calculated monoisotopic [M+2H]: 2109.7

Figure S13. VIQKI D455(β^3 D) MALDI-TOF MS analysisFigure S14. VIQKI D455(β^3 D) UPLC purity analysis, UPLC gradient from 10-95% MeCN/H₂O over 6 minutes (0.3 mL/min; column-Waters Acquity BEH C4 1.7 μ m, 2.1 x 100 mm, purity >95%)

VIQKI I456(β^3 I)Sequence: Ac-VALDPID(β^3 I)SIVLNKIKSQLEESKEWIRRSNKILDSI-NH₂

Calculated monoisotopic [M+H]: 4218.4

Calculated monoisotopic [M+2H]: 2109.7

Figure S15. VIQKI I456(β^3 I) MALDI-TOF MS analysisFigure S16. VIQKI I456(β^3 I) UPLC purity analysis, UPLC gradient from 10-95% MeCN/H₂O over 6 minutes (0.3 mL/min; column- Waters Acquity BEH C4 1.7 μ m, 2.1 x 100 mm, purity >95%)

Thermal Denaturation Assays for HPIV3 HRN+VIQKI β -variants

All circular dichroism (CD) spectroscopy experiments were performed on an Aviv Biomedical model 420 CD spectrometer. The CD spectrometer was calibrated with a 1 mg/mL solution of camphor sulfonic acid (CSA) in water. Samples were prepared in 1 mm quartz strain-free cuvettes (Hellma) using 50 μ M peptide in phosphate buffered saline (PBS). Spectra were collected from 260 nm to 202 nm with a 1 nm bandwidth and 5 second averaging time. For thermal denaturation experiments, ellipticity was measured at 222 nm as temperature was raised from 5–98 $^{\circ}$ C in 3-degree increments with a 5-minute equilibration time and a 5-second averaging time for each measurement. T_m values were determined as mean values of three replicates \pm standard deviation.

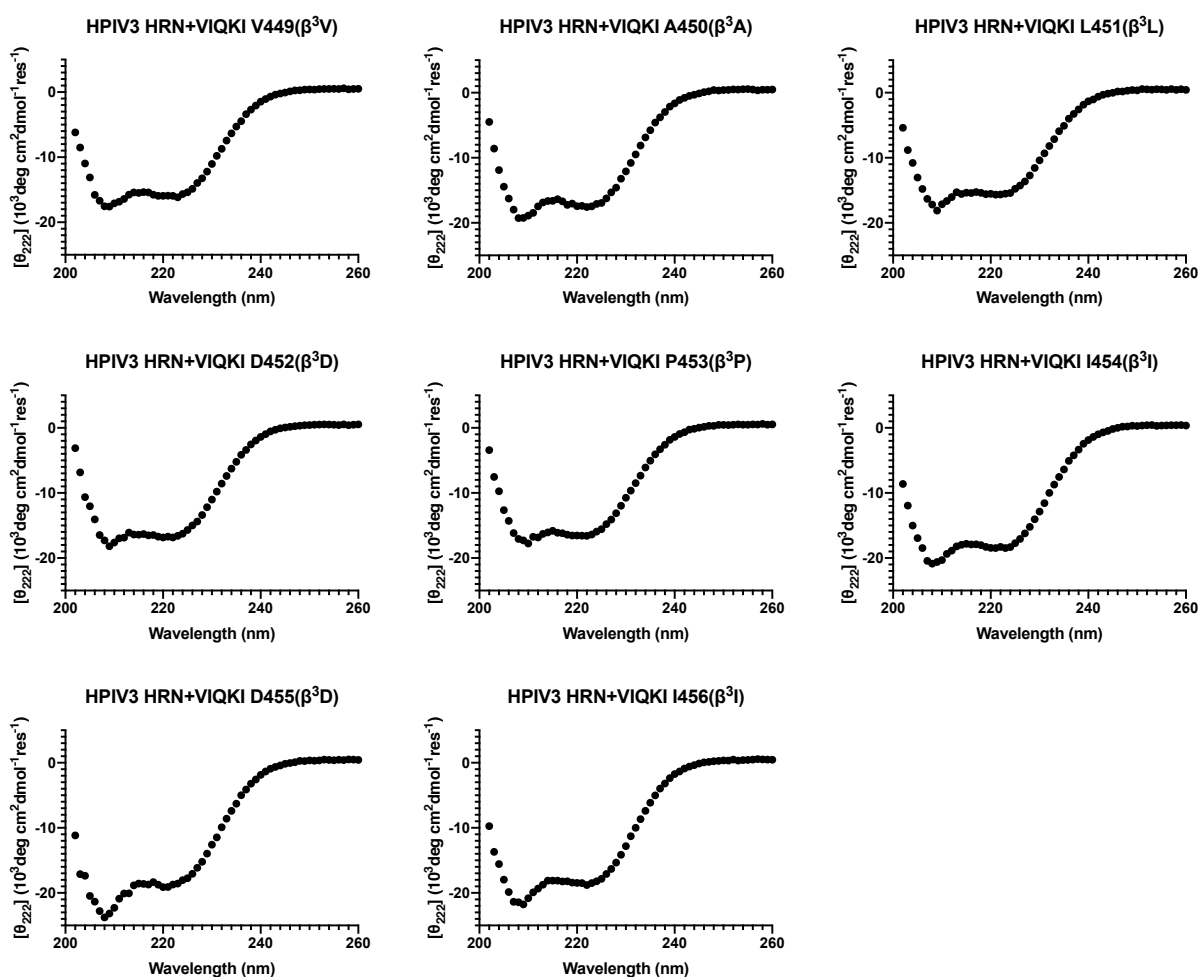


Figure S17 Circular dichroism spectra of 1:1 mixtures of HPIV3 HRN+VIQKI β -variants (23 $^{\circ}$ C, 50 μ M each peptide in PBS).

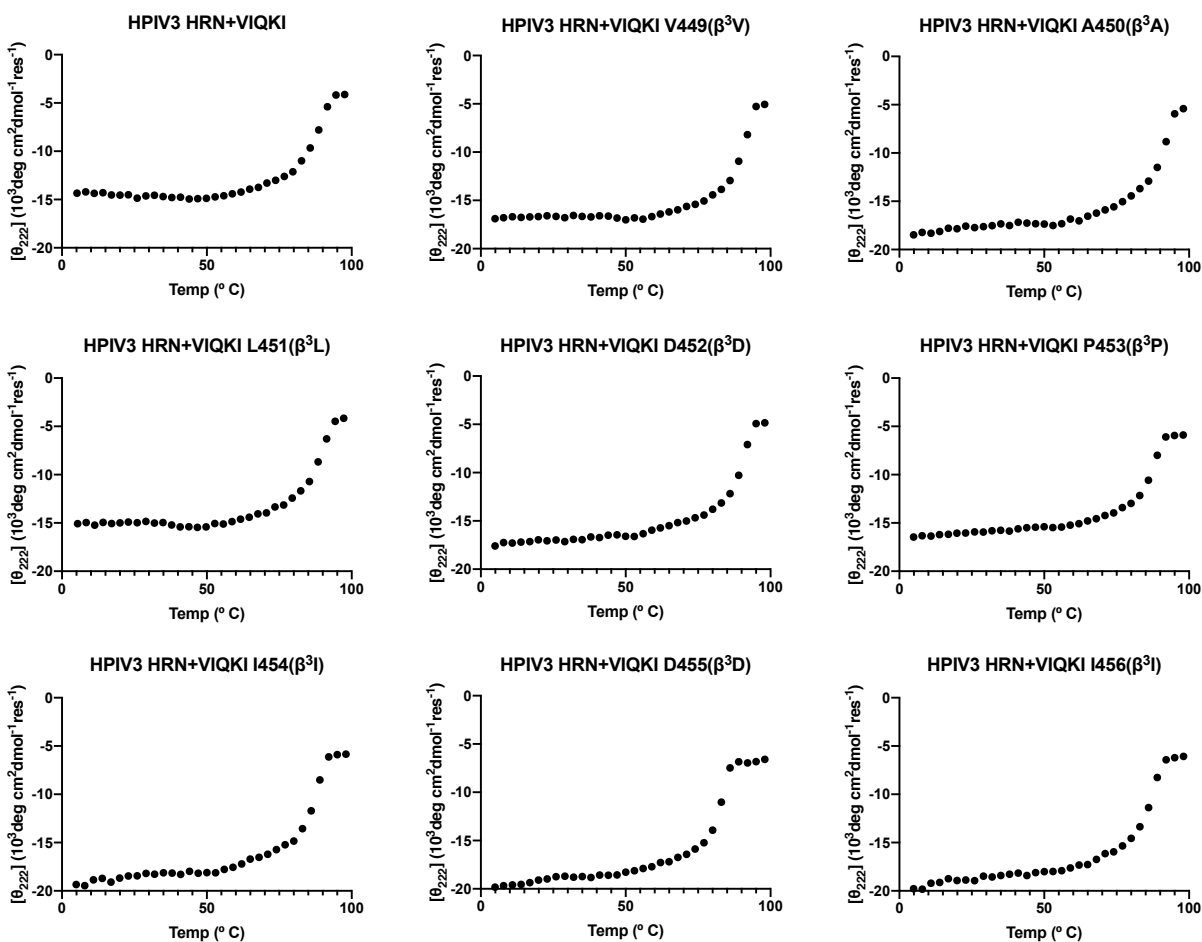


Figure S18 Thermal denaturation of 1:1 mixtures of HPIV3 HRN+VIQKI and VIQKI β -variants, 50 μ M each peptide, in PBS.

Assessment of Peptide Efficacy

Plasmids, Cells, and Viruses

HEK293T (human embryonic kidney), CV-1 and Vero E6 cells were obtained from ATCC and were grown in Dulbecco's modified Eagle's medium (DMEM; Gibco) supplemented with 10% fetal bovine serum and antibiotics at 37°C and 5% CO₂. All cells tested negative for mycoplasma in MycoAlert™ Mycoplasma Detection Kit (Lonza).

Antiviral Efficacy against Live RSV or HPIV3

Peptide activity against RSV or HPIV3 was determined by plaque reduction assays in infected cell monolayers as described previously.^{1,2} We used recombinant RSV that expresses green fluorescent protein (rgRSV) and recombinant HPIV3 that expresses enhanced green fluorescent protein (rHPIV3 CI-1-EGFP) so that infection could be quantified by fluorescence. For cell maintenance, HEp-2 cells (ATCC no. CCL-23) and Vero cells (ATCC no. CCL-81) were grown as monolayers and maintained in DMEM supplemented with 10% fetal bovine serum (FBS) and 2 mM L-glutamine in a humidified atmosphere with 5%CO₂ at 37 °C. Viral stocks were prepared in HEp-2 cells for rgRSV or CV-1 cells for rHPIV3. Briefly, HEp-2 cells and CV-1 cells were grown overnight, washed with OptiMEM, and inoculated with rgRSV or rHPIV3, respectively. After a 2.5-h adsorption period the cells were incubated for 3 days in DMEM supplemented with 2% FBS. HPIV3 was collected in supernatant fluids and stored at -80 °C. RSV was harvested by three freeze-thaw cycles followed by a clarifying centrifugation at 3,500 rpm. and stored at -80 °C. Viral titers were determined by plaque assay in Hep-2 cells using a 2% methyl cellulose overlay, 5% (v/v) formaldehyde fixation, at 48hpi as previously described^{1,2} and imaged on an In Cell Analyzer (GE). To quantify the effects of peptides on RSV or HPIV3 viral entry, Hep-2 cell monolayers grown in 96-well plates were incubated for 120 min with approximately 100 PFU of rgRSV or rHPIV3 in medium containing various concentrations of inhibitors. The medium was discarded and replaced by methylcellulose, and the cultures were incubated at 37°C for 48h. Fluorescence was quantitated on an In Cell Analyzer (GE).

X-ray Crystallography

Crystallization Conditions

Separate stock solutions of the HPIV3 HRN and VIQKI β -variant peptides were prepared by dissolving the lyophilized peptide powder in water. Peptide concentration was measured by UV absorbance using tryptophan and tyrosine as the chromophores. Co-crystallization solutions were then prepared by mixing equal molar amounts of the relevant individual peptide solutions. Crystals were grown using hanging drop vapor diffusion. A 2 μ L drop that comprised a 1:1 mixture of co-crystallization solution and the crystallization condition was placed on a glass cover slide that was then inverted to seal a well containing 150 μ L of the crystallization condition. The crystallization conditions are given below.

- HPIV3 HRN+VIQKI D452(β^3 D): 30 mM NaF; 30 mM NaBr; 30 mM NaI; 12.5% (v/v) 2-methyl-2,4-pentanediol; 12.5% (v/v) PEG 1000; 12.5% (w/v) PEG 3350; 100 mM NaHEPES/MOPS buffer (pH 7.5)
- HPIV3 HRN+VIQKI P453(β^3 P): 30 mM NaF; 30 mM NaBr; 30 mM NaI; 20% v/v PEG 500 MME; 10 % w/v PEG 20000; 100 mM imidazole/MES monohydrate (pH 6.5)
- HPIV3 HRN+VIQKI I454(β^3 I): 30 mM sodium nitrate; 30 mM dibasic sodium phosphate; 30 mM ammonium sulfate; 100 mM imidazole/MES monohydrate (pH 6.5); 12.5% PEG1000; 12.5% PEG3350; 12.5% 2-methyl-2,4-pentanediol
- HPIV3 HRN+VIQKI D455(β^3 D): 30 mM sodium nitrate; 30 mM dibasic sodium phosphate; 30 mM ammonium sulfate; 12.5% PEG1000; 12.5% PEG3350; 12.5% 2-methyl-2,4-pentanediol; 100 mM imidazole/MES monohydrate (pH 6.5)
- HPIV3 HRN+VIQKI I456(β^3 I): 30 mM sodium nitrate; 30 mM dibasic sodium phosphate; 30 mM ammonium sulfate; 12.5% PEG1000; 12.5% PEG3350; 12.5% 2-methyl-2,4-pentanediol; 100 mM NaHEPES/MOPS buffer (pH 7.5)

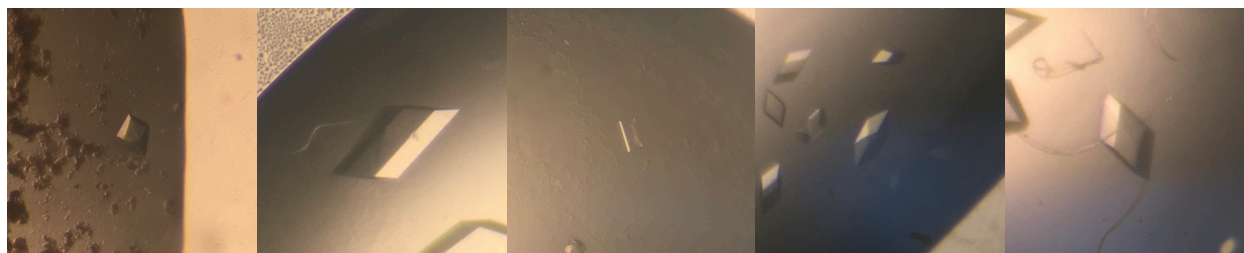


Figure S19 Crystal morphologies for (left to right) HPIV3 HRN+VIQKI D452(β^3 D), HPIV3 HRN+VIQKI P453(β^3 P), HPIV3 HRN+VIQKI I454(β^3 I), HPIV3 HRN+VIQKI D455(β^3 D), HPIV3 HRN+VIQKI I456(β^3 I),

X-ray Data Collection

Crystals were looped and vitrified in liquid nitrogen. Diffraction data was collected at the Life Sciences Collaborative Access Team (LS-CAT) beam line 21-ID-G at the Advanced Photon Source (APS) at Argonne National Laboratory (ANL).

Data Processing, Structure Solution, and Refinement

Data were indexed and integrated using the program *XDS*. Data were then scaled and merged using the program *XSCALE*.³ A molecular replacement solution was found with the program *Phaser* for each dataset using a truncated dimer consisting of chains A and B of HPIV3 HRN+VIQKI (PDB: 6NRO) as a search model. Chain A was truncated to residues 153–173, chain B was truncated to residues 460–480, and all side chains were removed prior to molecular replacement. Model refinement was carried out using the program *phenix.refine* in combination with manual real-space model building and refinement in the program *Coot*.^{4,5}

Table S2. HPIV3 HRN:VIQKI D452(β^3 D) (PDB: 6PZ6)

Data collection	
X-ray source	APS 21-ID-G
X-ray detector	MAR300
Detector distance (mm)	225
Oscillation range ($^\circ$)	0.5
Wavelength (\AA)	0.9786
Space group	P 1 2 ₁ 1
a / b / c (\AA)	39.6 / 52.5 / 55.6
α / β / γ ($^\circ$)	90 / 99.2 / 90
Matthews coefficient ($\text{\AA}^3/\text{Da}$)	2.09
Solvent content (%)	36.2
Resolution range (\AA)	27.45–1.70 (1.73–1.70)
Number of observations	183314 (8613)
Unique reflections	24510 (1206)
Completeness	98.44 % (98.29%)
Redundancy	7.5 (7.6)
Mean $I/\sigma(I)$	19.9 (1.0)
CC1/2*	1.00 (0.55)
R_{merge}	0.045 (1.809)
R_{meas}	0.049 (1.940)
R_{pim}	0.018 (0.698)
Wilson B-factor (\AA^2)	36.94
Refinement statistics	
Refinement program	Phenix.refine: 1.13-2998
Resolution range (\AA)	27.45–1.70 (1.74–1.70)
No. of unique reflections used in refinement	24500 (1580)
Completeness (%)	98.40% (97.56%)
Reflections in cross-validation set	1999
R-value (work)	22.8
R-value (free)	25.4
R-value (overall)	23.0
Coordinate error (ML, \AA)	0.24
Mean ADP (\AA^2)	63.51

Table S3. HPIV3 HRN:VIQKI P453(β^3 P) (PDB: 6PRL)

Data collection	
X-ray source	APS 21-ID-G
X-ray detector	MAR300
Detector distance (mm)	225
Oscillation range ($^{\circ}$)	0.5
Wavelength (\AA)	0.9786
Space group	P 1 2 ₁ 1
a / b / c (\AA)	35.5 / 53.2 / 58.2
α / β / γ ($^{\circ}$)	90.0 / 90.1 / 90.0
Matthews coefficient ($\text{\AA}^3/\text{Da}$)	1.95
Solvent content (%)	37.0
Resolution range (\AA)	39.26–1.87 (1.937–1.87)
Number of observations	124514
Unique reflections	17950 (1687)
Completeness	98.82% (93.35%)
Redundancy	6.9 (4.9)
Mean $I/\sigma(I)$	8.57 (1.99)
CC1/2*	0.97 (0.46)
R_{merge}	0.2746 (2.765)
R_{meas}	0.2977 (3.064)
R_{pim}	0.1134 (1.281)
Wilson B-factor (\AA^2)	12.96
Refinement statistics	
Refinement program	Phenix.refine: 1.13-2998
Resolution range (\AA)	39.26–1.87 (1.92–1.87)
No. of unique reflections used in refinement	17845
Completeness (%)	98.80% (91.40%)
Reflections in cross-validation set	1781
R-value (work)	20.3
R-value (free)	25.1
R-value (overall)	20.7
Coordinate error (ML, \AA)	0.23
Mean ADP (\AA^2)	28.4

Table S4. HPIV3 HRN:VIQKI I454(β^3 I) (PDB: 6VAS)

Data collection	
X-ray source	APS 21-ID-G
X-ray detector	MAR300
Detector distance (mm)	180
Oscillation range ($^{\circ}$)	0.5
Wavelength (\AA)	0.9786
Space group	P 3 2 1
a / b / c (\AA)	50.6 / 50.6 / 76.1
α / β / γ ($^{\circ}$)	90 / 90 / 120
Matthews coefficient ($\text{\AA}^3/\text{Da}$)	1.43
Solvent content (%)	13.8
Resolution range (\AA)	28.73–1.49 (1.543–1.49)
Number of observations	399707
Unique reflections	18936 (1814)
Completeness	99.65% (98.53%)
Redundancy	21.1 (21.7)
Mean $I/\sigma(I)$	15.96 (1.63)
CC1/2*	1.00 (0.68)
R_{merge}	0.105 (2.045)
R_{meas}	0.108 (2.094)
R_{pim}	0.0238 (0.4476)
Wilson B-factor (\AA^2)	22.87
Refinement statistics	
Refinement program	Phenix.refine: 1.17.1_3660
Resolution range (\AA)	28.73–1.49 (1.53–1.49)
No. of unique reflections used in refinement	18929
Completeness (%)	99.65 (98.01)
Reflections in cross-validation set	1886
R-value (work)	24.5
R-value (free)	26.2
R-value (overall)	24.6
Coordinate error (ML, \AA)	0.20
Mean ADP (\AA^2)	41.61

Table S5. HPIV3 HRN:VIQKI D455(β^3 D) (PDB: 6PYQ)

Data collection	
X-ray source	APS 21-ID-G
X-ray detector	MAR300
Detector distance (mm)	225
Oscillation range ($^\circ$)	0.5
Wavelength (\AA)	0.9786
Space group	P 1 2 ₁ 1
a / b / c (\AA)	39.9 / 49.3 / 56.2
α / β / γ ($^\circ$)	90 / 103.6 / 90
Matthews coefficient ($\text{\AA}^3/\text{Da}$)	1.81
Solvent content (%)	32.18
Resolution range (\AA)	24.73–1.79 (1.82–1.79)
Number of observations	170050
Unique reflections	20102 (1037)
Completeness	99.76% (99.71%)
Redundancy	8.5 (8.6)
Mean $I/\sigma(I)$	13.7 (1.0)
CC1/2*	1.00 (0.40)
R_{merge}	0.084 (2.021)
R_{meas}	0.089 (2.151)
R_{pim}	0.031 (0.732)
Wilson B-factor (\AA^2)	29.85
Refinement statistics	
Refinement program	Phenix.refine: 1.13-2998
Resolution range (\AA)	24.73–1.79 (1.83–1.79)
No. of unique reflections used in refinement	20082
Completeness (%)	99.66 (99.79)
Reflections in cross-validation set	1998
R-value (work)	20.7
R-value (free)	23.2
R-value (overall)	20.9
Coordinate error (ML, \AA)	0.19
Mean ADP (\AA^2)	49.58

Table S6. HPIV3 HRN:VIQKI I456(β^3 I) (PDB: 6V3V)

Data collection	
X-ray source	APS 21-ID-G
X-ray detector	MAR300
Detector distance (mm)	300
Oscillation range ($^{\circ}$)	0.5
Wavelength (\AA)	0.9786
Space group	P 1 2 ₁ 1
a / b / c (\AA)	39.3 / 52.3 / 56.7
α / β / γ ($^{\circ}$)	90 / 98.4 / 90
Matthews coefficient ($\text{\AA}^3/\text{Da}$)	1.94
Solvent content (%)	36.74
Resolution range (\AA)	28.02–2.17 (2.248–2.17)
Number of observations	90915
Unique reflections	12097 (1195)
Completeness	99.5% (99.5%)
Redundancy	7.5 (7.5)
Mean $I/\sigma(I)$	15.31 (1.17)
CC1/2*	1.00 (0.52)
R_{merge}	0.067 (1.87)
R_{meas}	0.072 (2.008)
R_{pim}	0.026 (0.7275)
Wilson B-factor (\AA^2)	52.31
Refinement statistics	
Refinement program	Phenix.refine: 1.17.1_3660
Resolution range (\AA)	28.02–2.17 (2.26–2.17)
No. of unique reflections used in refinement	12097
Completeness (%)	99.5 (99.6)
Reflections in cross-validation set	1209
R-value (work)	24.1
R-value (free)	28.8
R-value (overall)	24.5
Coordinate error (ML, \AA)	0.36
Mean ADP (\AA^2)	76.63

References

1. Outlaw, V. K.; Bottom-Tanzer, S.; Kreitler, D. F.; Gellman, S. H.; Porotto, M.; Moscona, A. Dual Inhibition of Human Parainfluenza Type 3 and Respiratory Syncytial Virus Infectivity with a Single Agent. *J. Am. Chem. Soc.* **2019**, *141* (32), 12648–12656.
2. Palmer, S. G.; DeVito, I.; Jenkins, S. G.; Niewiesk, S.; Porotto, M.; Moscona, A. Circulating Clinical Strains of Human Parainfluenza Virus Reveal Viral Entry Requirements for in Vivo Infection. *J. Virol.* **2014**, *88* (22), 13495–13502.
3. Kabsch, W. (2010) Integration, scaling, space-group assignment and post-refinement. *Acta Crystallogr. D Biol. Crystallogr.* *66*:125-132.
4. Adams, P. D.; Afonine, P. V.; Bunkóczi, G.; Chen, V. B.; Davis, I. W.; Echols, N.; Headd, J. J.; Hung, L.-W.; Kapral, G. J.; Grosse-Kunstleve, R. W.; McCoy, A. J.; Moriarty, N. W.; Oeffner, R.; Read, R. J.; Richardson, D. C.; Richardson, J. S.; Terwilliger, T. C.; Zwart, P. H. PHENIX: a Comprehensive Python-Based System for Macromolecular Structure Solution. *Acta Crystallogr. D Biol. Crystallogr.* **2010**, *66* (2), 213–221.
5. Emsley, P.; Cowtan, K. Coot: Model-Building Tools for Molecular Graphics. *Acta Crystallogr. D Biol. Crystallogr.* **2004**, *60* (Pt 12 Pt 1), 2126–2132.